Stony Brook University | The State University of New York

Workshop "Exploring Quark-Gluon Plasma through soft and hard probes"

Nuclear shape imaging in high-energy nuclear collisions

Jiangyong Jia

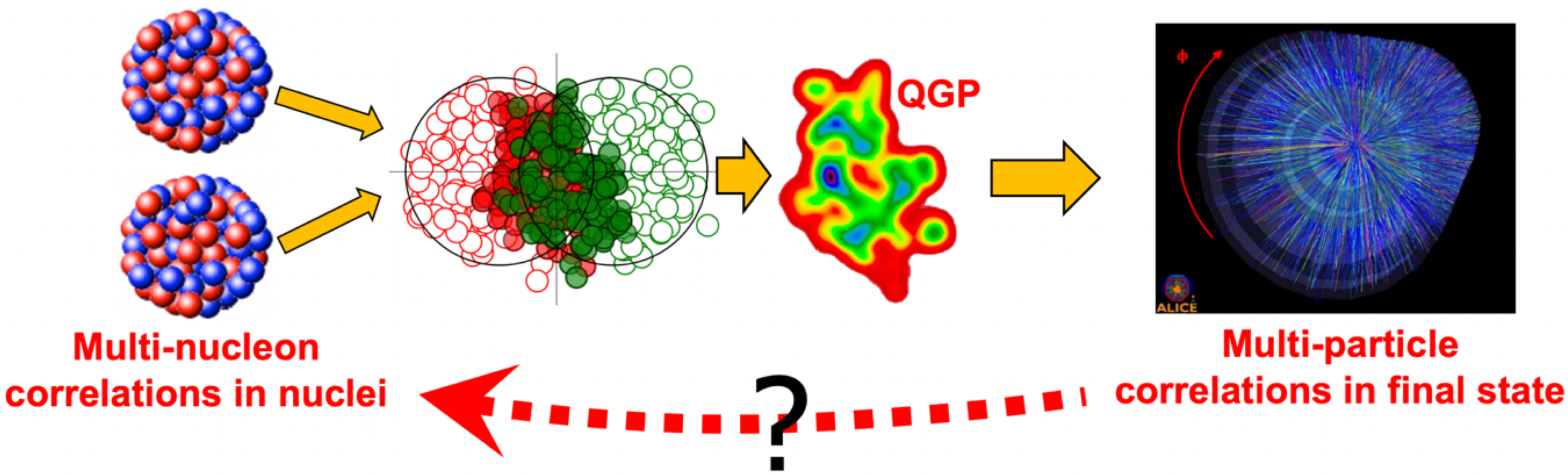

Brookhaven National Laboratory
Office of Science | U.S. Department of Energy

05/29/2023 - 05/31/2023

BROOKHAVEN NATIONAL LABORATORY

Collective shape of atomic nuclei

- Emergent phenomena of many-body quantum system
  - clustering, halo, skin, bubble…
  - quadrupole/octupole/hexdecopole deformations
  - Nontrivial evaluation with N and Z.

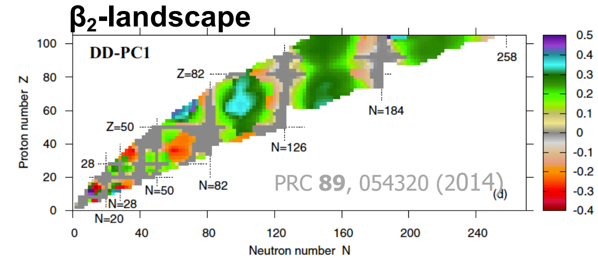

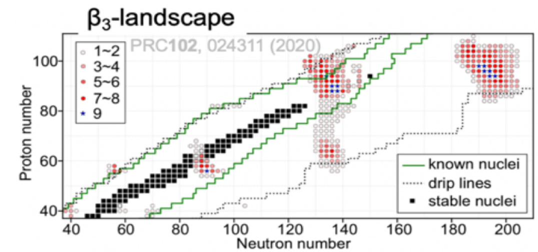

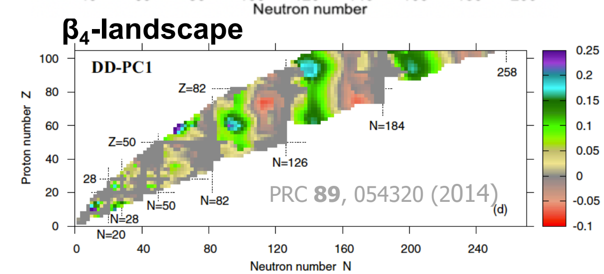

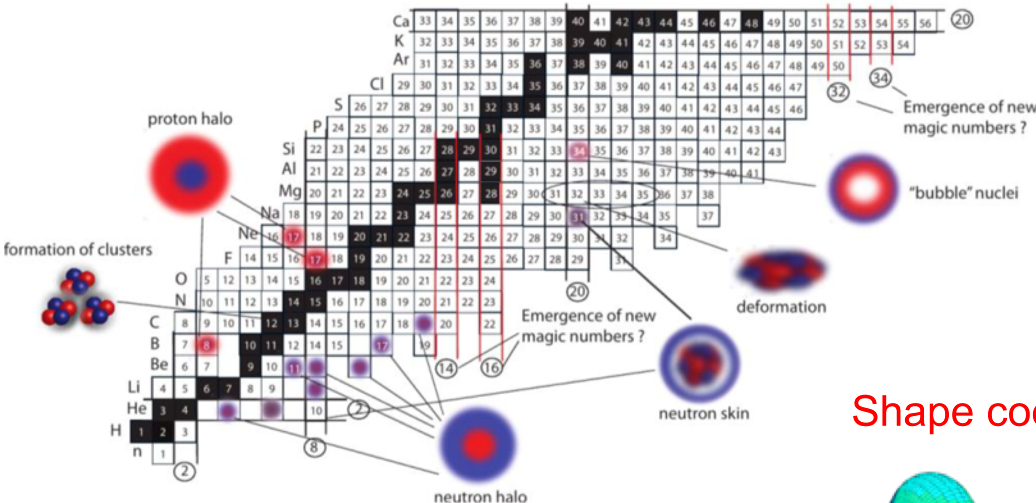

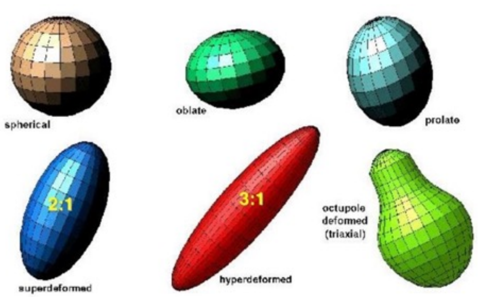

Shape coexistence

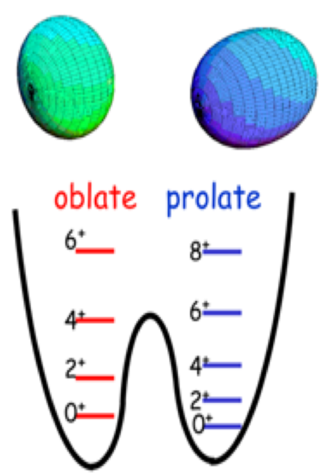

Two level model $|0_i^+\rangle = a|0_1^+\rangle + b\,|0_2^+\rangle$

$$|0_f^+\rangle = -b|0_1^+\rangle + a\,|0_2^+\rangle$$

$$\rho_{fi}(E0) \cong \frac{1}{eR^2}\left[ab\left(\langle 0_1^+|\hat{T}(E0)|0_1^+\rangle - \langle 0_2^+|\hat{T}(E0)|0_2^+\rangle\right)\right]$$

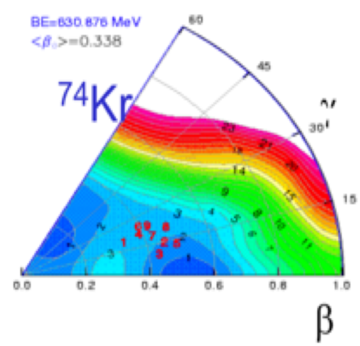

High-energy heavy ion collision

Nuclear structure

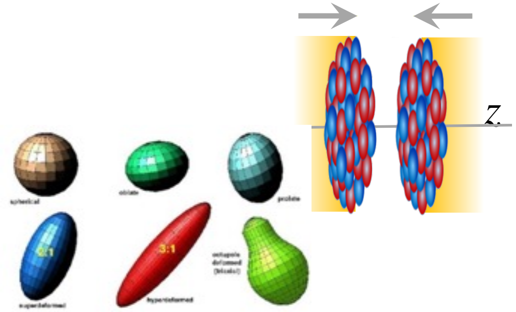

Shape and radial dis.

$\beta_2 \rightarrow$ Quadrupole deformation

$\beta_3 \rightarrow$ Octupole deformation

$a_0 \rightarrow$ Surface diffuseness

$R_0 \rightarrow$ Nuclear size

Initial condition

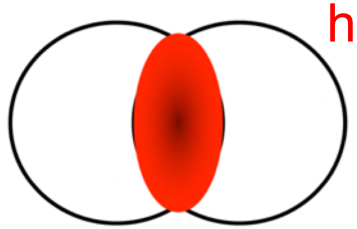

Volume, size and shape

N_{part}

$R_\perp^2 \propto \langle r_\perp^2 \rangle,$

$\mathcal{E}_n \propto \langle r_\perp^n e^{in\phi} \rangle$

hydrodynamics

Final state

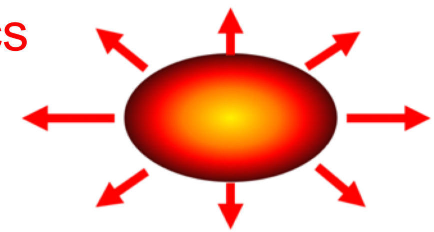

Observables

$$\frac{d^2N}{d\phi dp_T} = N(p_T)\left(\sum_n V_n\, e^{-in\phi}\right)$$

Extraction of QGP properties is limited by the uncertainties in initial condition

- Comparing collisions of nuclei with different shapes constrains the initial condition
- Provide insights on manifestation of nuclear structure at high energy scale.

Flow assisted imaging of the initial condition

Initial condition

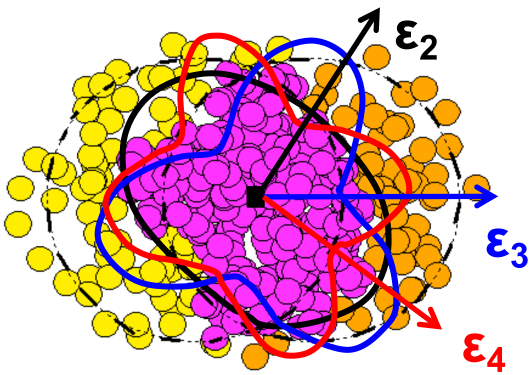

$$F = -\nabla P(\epsilon)$$

Hydro-response

Final Particle flow

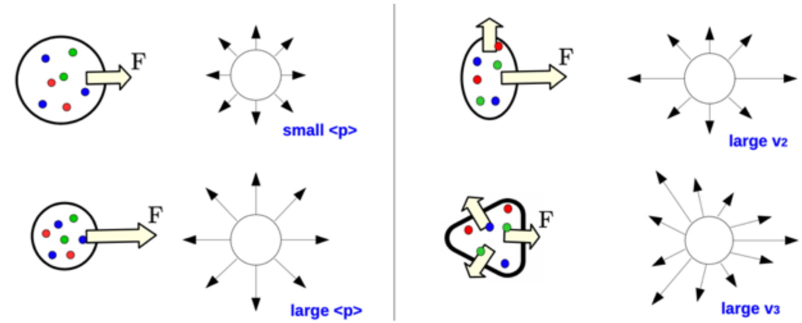

volume, size and shape

N_{part} $\quad R_\perp^2 \propto \langle r_\perp^2 \rangle,$

$$\mathcal{E}_2 \propto \left\langle r_\perp^2 \, e^{i2\phi} \right\rangle$$
$$\mathcal{E}_3 \propto \left\langle r_\perp^3 \, e^{i3\phi} \right\rangle$$
$$\mathcal{E}_4 \propto \left\langle r_\perp^4 \, e^{i4\phi} \right\rangle$$
$$\ldots$$

Multiplicity Radial Flow Harmonic Flow

N_{ch}

$$\frac{d^2N}{d\phi dp_T} = N(p_T)\left(\sum_n V_n \, e^{-in\phi}\right)$$

Flow assisted imaging of the initial condition

Initial condition

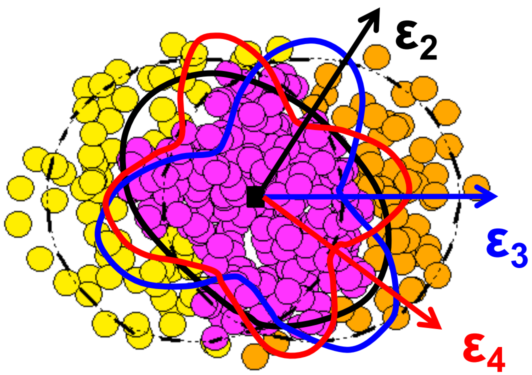

$$F = -\nabla P(\epsilon)$$

Hydro-response

Final Particle flow

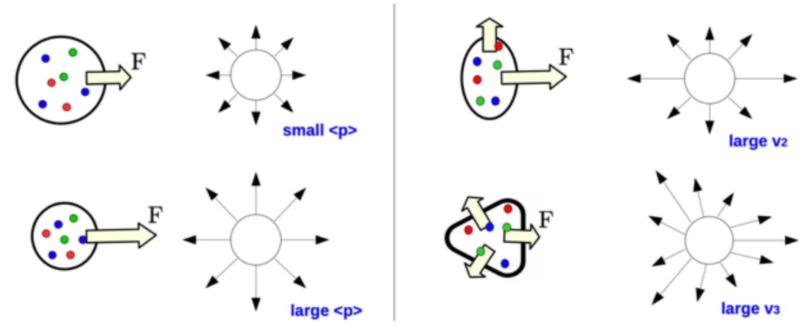

volume, size and shape

N_{part} $\quad R_\perp^2 \propto \langle r_\perp^2 \rangle,$

$$\mathcal{E}_2 \propto \left\langle r_\perp^2 e^{i2\phi} \right\rangle$$
$$\mathcal{E}_3 \propto \left\langle r_\perp^3 e^{i3\phi} \right\rangle$$
$$\mathcal{E}_4 \propto \left\langle r_\perp^4 e^{i4\phi} \right\rangle$$

Multiplicity Radial Flow Harmonic Flow

N_{ch}

$$\frac{d^2N}{d\phi dp_T} = N(p_T)\left(\sum_n V_n\, e^{-in\phi}\right)$$

Radial flow

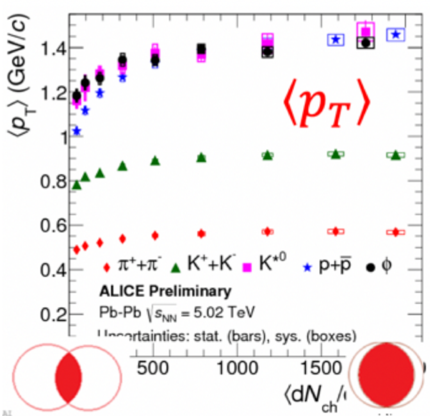

Elliptic flow

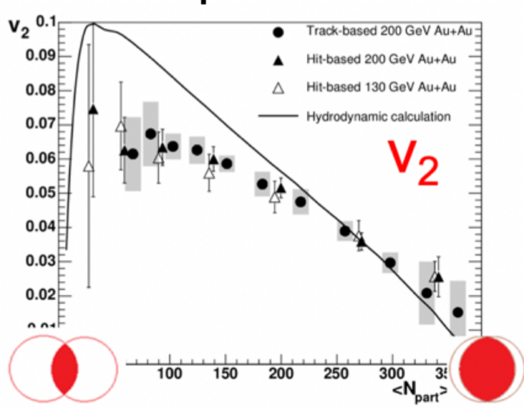

arXiv:1206.1905

Advantage of High energy:
⇒Large multiplicity and boost invariance
⇒approx. linear response in each event

$$N_{ch} \propto N_{part} \qquad \frac{\delta[p_T]}{[p_T]} \propto -\frac{\delta R_\perp}{R_\perp} \qquad V_n \propto \mathcal{E}_n$$

Connecting HI initial condition with nuclear shape

Body-Body

$$\mathcal{E}_2 = \epsilon_2 e^{i2\Phi} \propto \left\langle \boldsymbol{r}_\perp^2 e^{i2\phi} \right\rangle$$

Tip-Tip

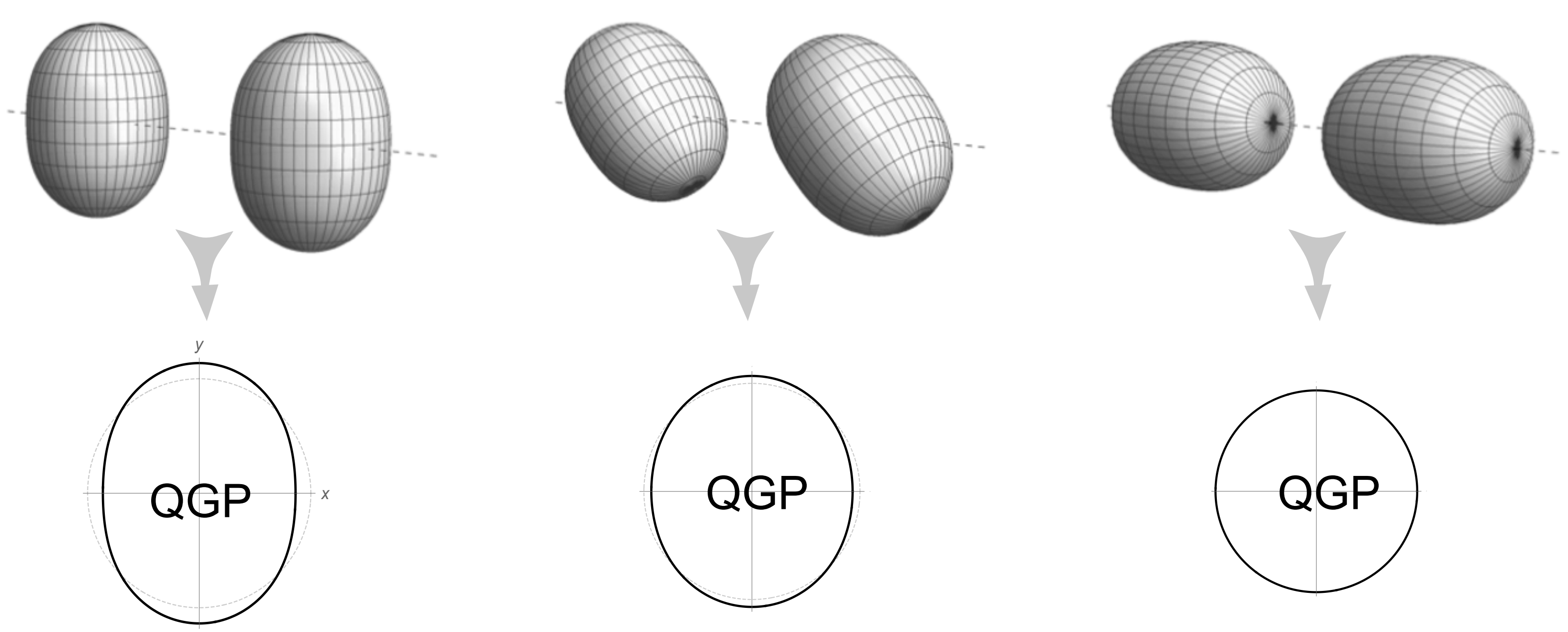

$\varepsilon_2 \sim 0.95\beta_2$

$\varepsilon_2 \sim 0.48\beta_2$

$\varepsilon_2 \sim 0$

$$\epsilon_2 = \underbrace{\epsilon_0}_{\text{undeformed}} + \underbrace{\boldsymbol{p}(\Omega_1, \Omega_2)}_{\text{phase factor}} \beta_2 + \mathcal{O}(\beta_2^2) \Longrightarrow \left\langle \epsilon_2^2 \right\rangle \approx \left\langle \epsilon_0^2 \right\rangle + 0.2\beta_2^2$$

$$\left\langle v_n^2 \right\rangle \propto \left\langle \epsilon_n^2 \right\rangle$$

Shape depends on Euler angle $\Omega = \varphi\theta\psi$

Intrinsic frame

Impact on high-order fluctuations

$$\rho(r,\theta,\phi) = \frac{\rho_0}{1+e^{(r-R(\theta,\phi))/a_0}} \quad R(\theta,\phi) = R_0\left(1+\beta_2[\cos\gamma Y_{2,0}+\sin\gamma Y_{2,2}]+\beta_3\sum_{m=-3}^{3}\alpha_{3,m}Y_{3,m}+\beta_4\sum_{m=-4}^{4}\alpha_{4,m}Y_{4,m}\right)$$

- In principle, can measure any moments of p(1/R, ε_2, ε_3…)
  - Mean $\langle d_\perp\rangle$ $\quad d_\perp \equiv 1/R_\perp$ $\quad\Rightarrow\quad \langle p_{\mathrm{T}}\rangle$
  - Variances: $\langle\varepsilon_n^2\rangle$, $\left\langle(\delta d_\perp/d_\perp)^2\right\rangle$ $\quad\Rightarrow\quad \langle v_n^2\rangle$, $\left\langle(\delta p_{\mathrm{T}}/p_{\mathrm{T}})^2\right\rangle$
  - Skewness $\langle\varepsilon_n^2\delta d_\perp/d_\perp\rangle$, $\left\langle(\delta d_\perp/d_\perp)^3\right\rangle$ $\quad\Rightarrow\quad \langle v_n^2\delta p_{\mathrm{T}}/p_{\mathrm{T}}\rangle$, $\left\langle(\delta p_{\mathrm{T}}/p_{\mathrm{T}})^3\right\rangle$
  - Kurtosis $\langle\varepsilon_n^4\rangle-2\langle\varepsilon_n^2\rangle^2$, $\left\langle(\delta d_\perp/d_\perp)^4\right\rangle-3\left\langle(\delta d_\perp/d_\perp)^2\right\rangle^2$ $\quad\Rightarrow\quad \langle v_n^4\rangle-2\langle v_n^2\rangle^2$, $\left\langle(\delta p_{\mathrm{T}}/p_{\mathrm{T}})^4\right\rangle-3\left\langle(\delta p_{\mathrm{T}}/p_{\mathrm{T}})^2\right\rangle^2$

  …
- All have simple connection to deformation:
  - Variances

$$\begin{aligned}
\langle\varepsilon_2^2\rangle &\sim a_2+b_2\beta_2^2\\
\langle\varepsilon_3^2\rangle &\sim a_3+b_3\beta_3^2\\
\langle\varepsilon_4^2\rangle &\sim a_4+b_4\beta_4^2+b_{4,2}\beta_2^2\\
\left\langle(\delta d_\perp/d_\perp)^2\right\rangle &\sim a_0+b_0\beta_2^2+b_{0,3}\beta_3^2
\end{aligned}$$

  - Skewness

$$\begin{aligned}
\left\langle\varepsilon_2^2\delta d_\perp/d_\perp\right\rangle &\sim a_1-b_1\cos(3\gamma)\beta_2^3\\
\left\langle(\delta d_\perp/d_\perp)^3\right\rangle &\sim a_2+b_2\cos(3\gamma)\beta_2^3
\end{aligned}$$

Low-energy vs high-energy method

- One-body distribution seen in lab-frame is always spherical, deformation appears as broadening of nucleon distribution
- Intrinsic frame quadrupole moment also accessible via sum rule or laser spectroscopy

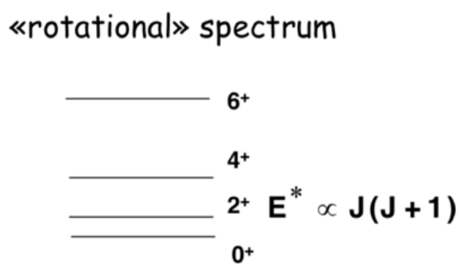

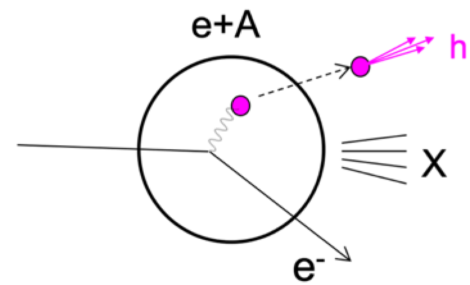

- Shape frozen in nuclear crossing (10^{-24}s <<rotational time scale 10^{-21}s), probe entire mass distribution via multi-point correlations.

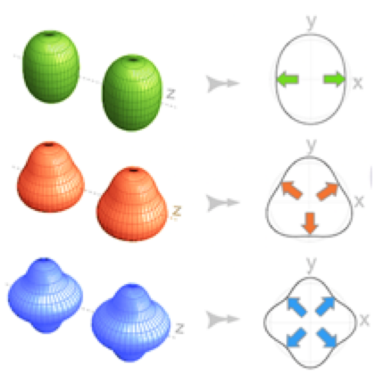

Collective flow response to nuclear shape

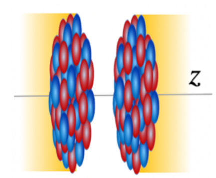

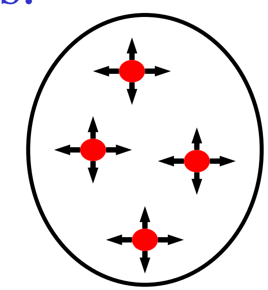

1902.07168

$\mathbf{r} = re^{i\phi}$

$$S(\mathbf{r}_1, \mathbf{r}_2) = \langle \rho(\mathbf{r}_1)\rho(\mathbf{r}_2)\rangle - \langle \rho(\mathbf{r}_1)\rangle\langle \rho(\mathbf{r}_2)\rangle$$

$$\epsilon_2 = \frac{\int_{\mathbf{r}} \mathbf{r}^2 S(\mathbf{r})}{\int_{\mathbf{r}} |\mathbf{r}|^2 \langle S(\mathbf{r})\rangle} \Rightarrow \langle \varepsilon_2^2 \rangle = \frac{\int_{\mathbf{r}_1,\mathbf{r}_2} (\mathbf{r}_1)^2 (\mathbf{r}_2^*)^2 S(\mathbf{r}_1,\mathbf{r}_2)}{\left(\int_{\mathbf{r}} |\mathbf{r}|^2 \langle S(\mathbf{r})\rangle\right)^2}$$

Digression: molecular structure imaging

Coulomb Explosion Imaging

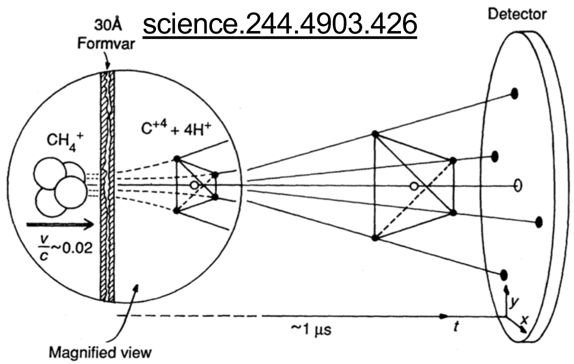

Fig. 1. A schematic view of a Coulomb explosion experiment. When a swift molecule passes through a thin solid film, it loses all of its binding electrons. The remaining positive ions repel each other, thus transforming the microstructure (as seen in the magnified view) into a macrostructure that can be measured precisely with an appropriate detector. The measured traces (*x*, *y*, *t*) of each fragment nucleus for individual molecules are then transformed into the original molecular structure.

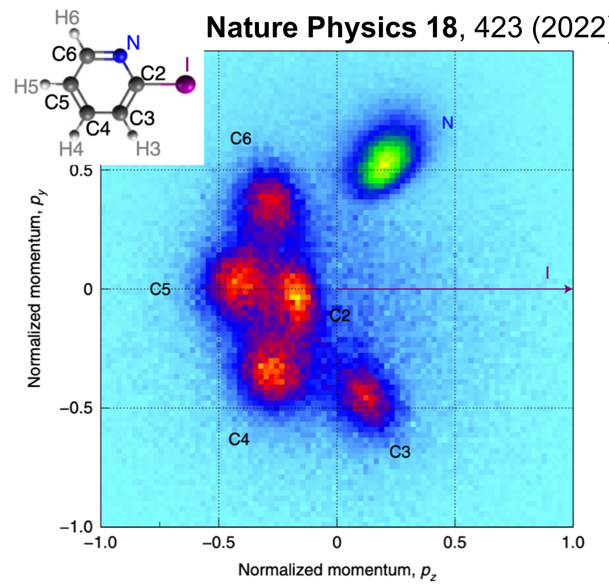

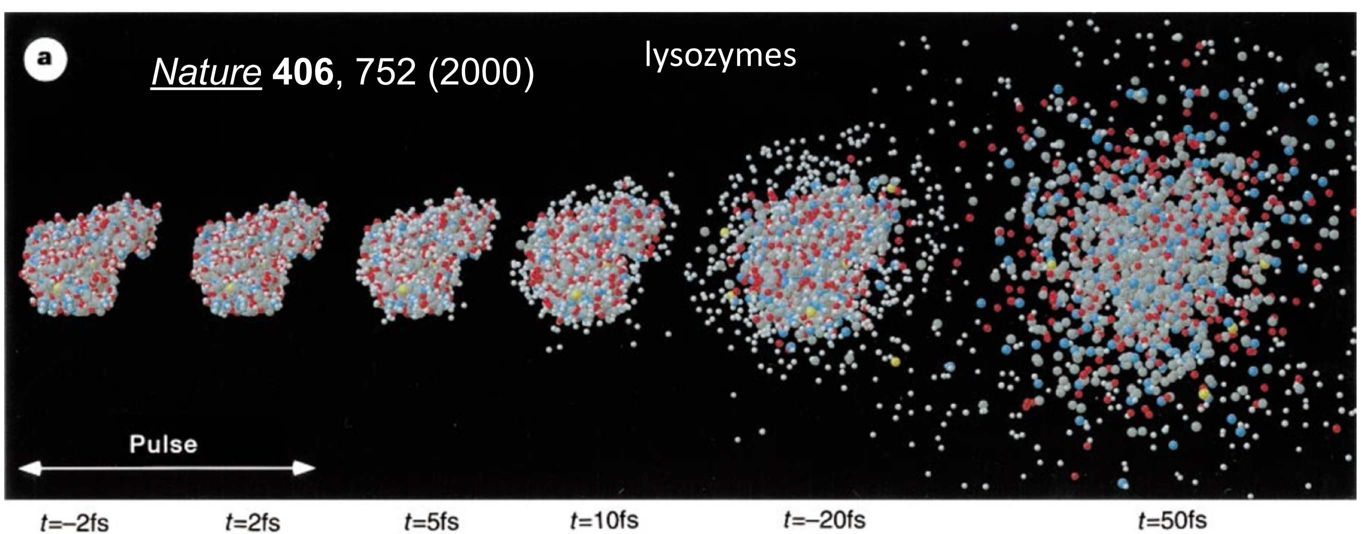

Strategy for nuclear shape imaging

Flow observable = k ⊗ initial condition (structure)

QGP response,
a smooth function of N+Z

Structure of colliding nuclei,
non-monotonic function of N and Z

QGP

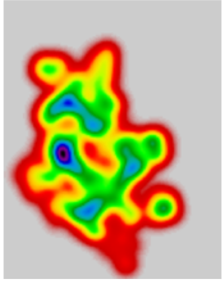

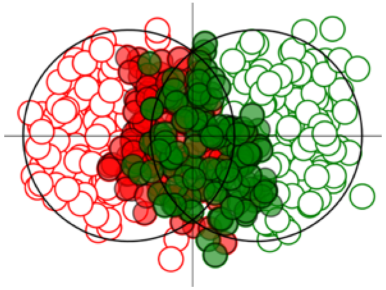

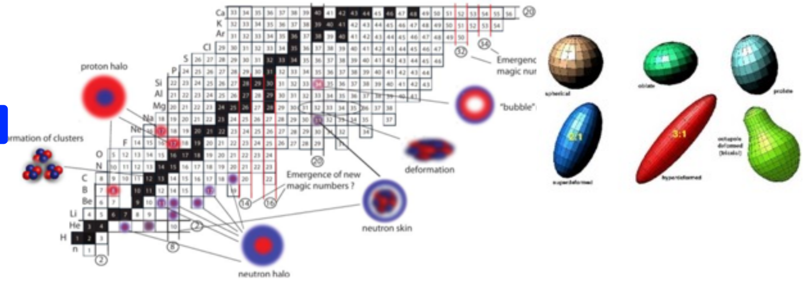

See 2209.11042 for more discussion

Case study: Isobar collisions at RHIC

^{96}Ru+^{96}Ru and ^{96}Zr+^{96}Zr at $\sqrt{s_{NN}}$ =200 GeV

- A key question for any HI observable O:

$$\frac{O_{^{96}\mathrm{Ru}+^{96}\mathrm{Ru}}}{O_{^{96}\mathrm{Zr}+^{96}\mathrm{Zr}}} \stackrel{?}{=} 1$$

Deviation from 1 must has origin in the nuclear structure, which impacts the initial state and then survives to the final state.

- Expectation

2109.00131

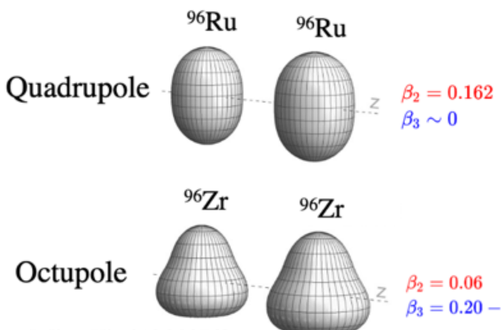

J. Jia, aXiv:2106.08768

$$\mathcal{O} \approx b_0 + b_1\beta_2^2 + b_2\beta_3^2 + b_3(R_0 - R_{0,\mathrm{ref}}) + b_4(a - a_{\mathrm{ref}})$$

$$R_{\mathcal{O}} \equiv \frac{\mathcal{O}_{\mathrm{Ru}}}{\mathcal{O}_{\mathrm{Zr}}} \approx 1 + c_1\Delta\beta_2^2 + c_2\Delta\beta_3^2 + c_3\Delta R_0 + c_4\Delta a$$

Species	β_2	β_3	a_0	R_0
Ru	0.162	0	0.46 fm	5.09 fm
Zr	0.06	0.20	0.52 fm	5.02 fm
difference	$\Delta\beta_2^2$	$\Delta\beta_3^2$	Δa_0	ΔR_0
	0.0226	-0.04	-0.06 fm	0.07 fm

Structure influences everywhere

$$R_{\mathcal{O}} \equiv \frac{\mathcal{O}_{\mathrm{Ru}}}{\mathcal{O}_{\mathrm{Zr}}}$$

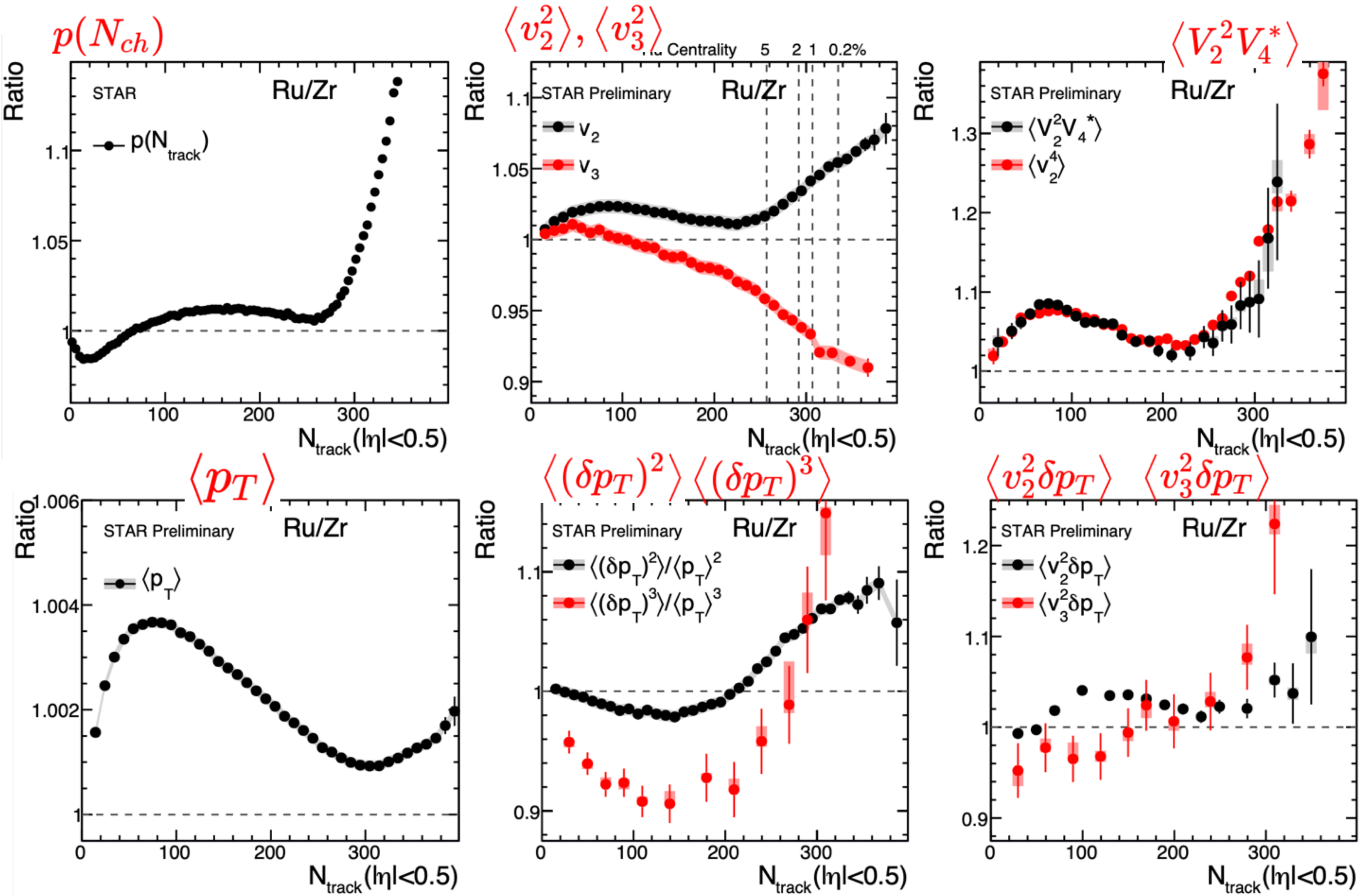

Nuclear structure via v_2-ratio and v_3-ratio

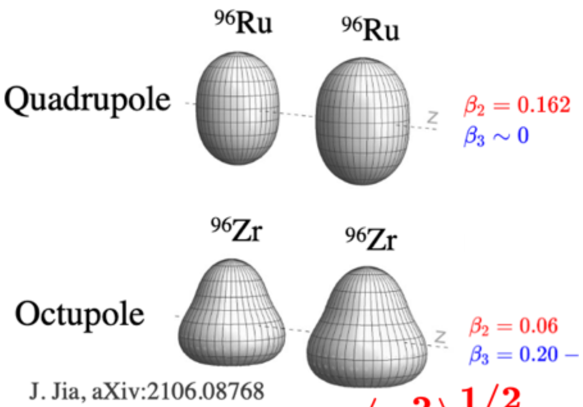

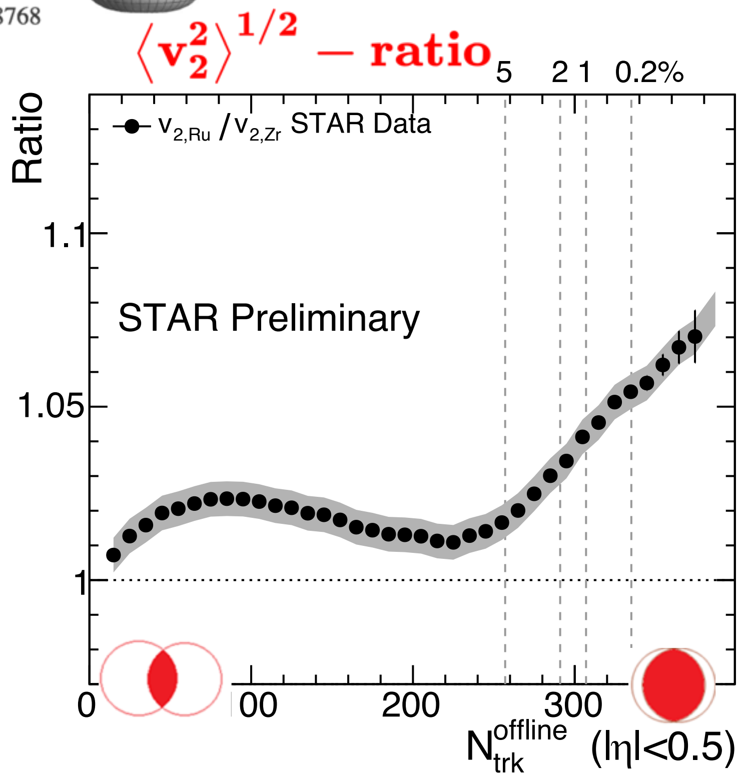

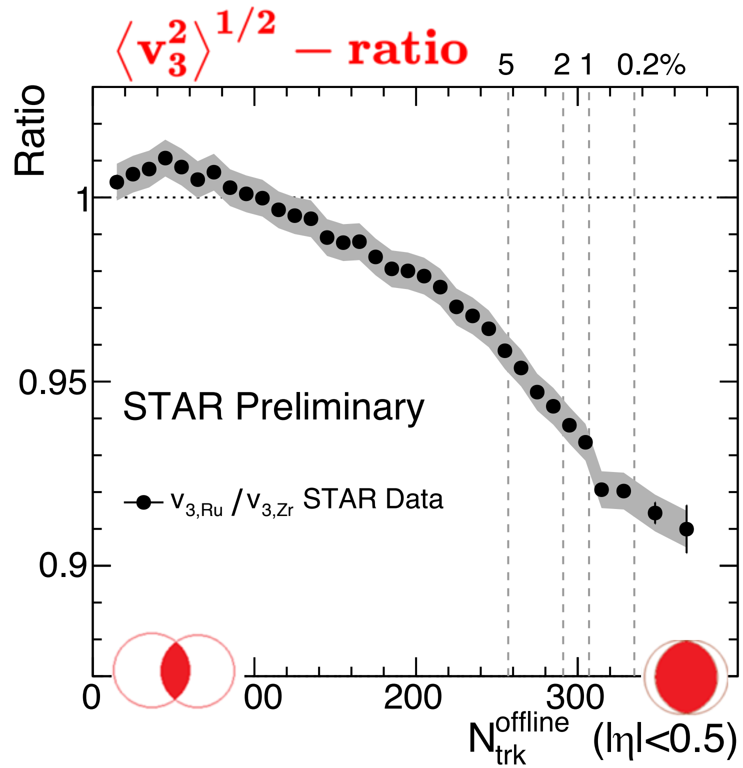

Nuclear structure via v_2-ratio and v_3-ratio

- β_{2Ru}~0.16 increase v_2, no influence on v_3 ratio

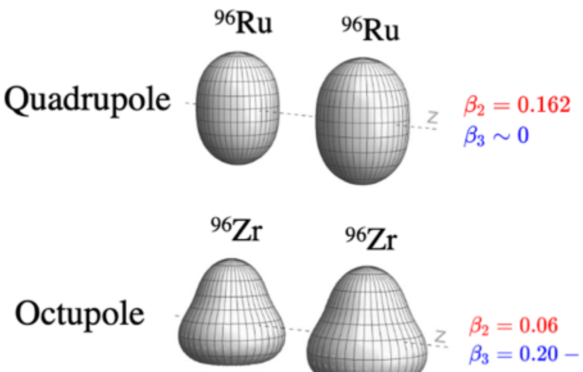

J. Jia, aXiv:2106.08768

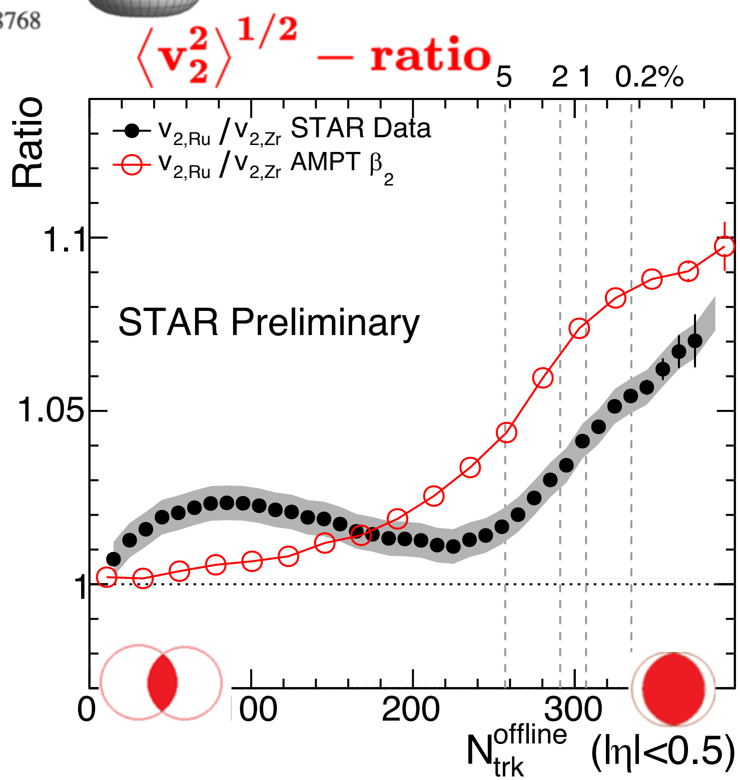

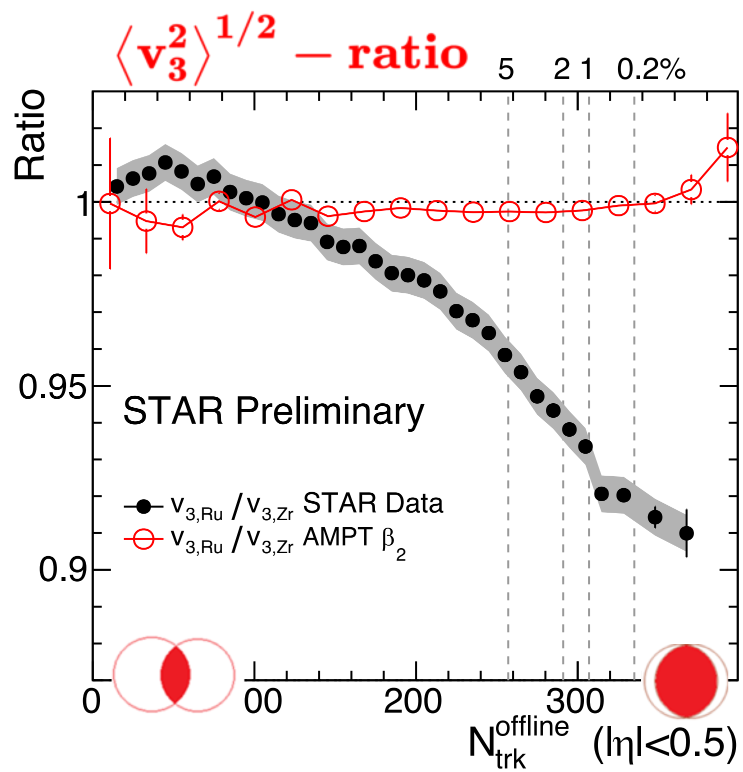

Nuclear structure via v_2-ratio and v_3-ratio

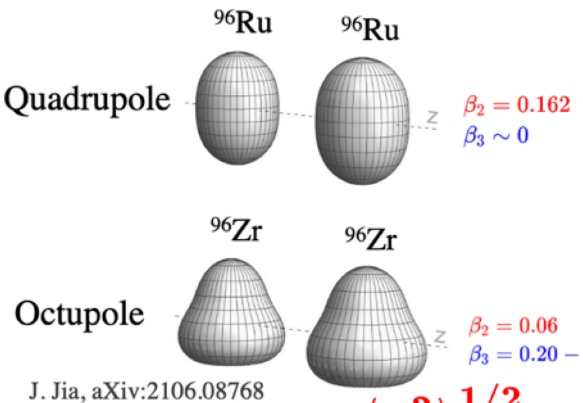

- β_{2Ru}~0.16 increase v_2, no influence on v_3 ratio
- β_{3Zr}~0.2 decrease v_2 in mid-central, decrease v_3 ratio

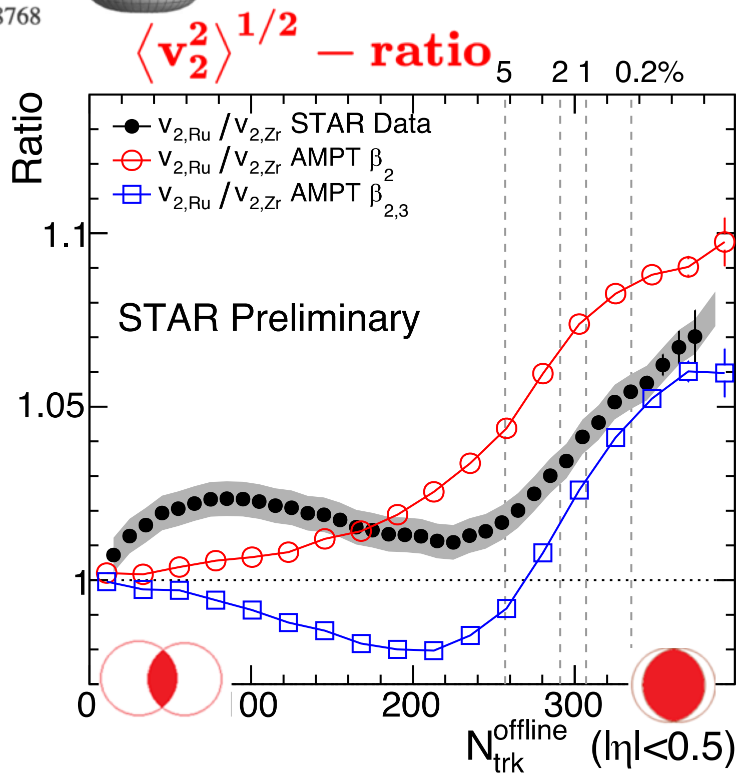

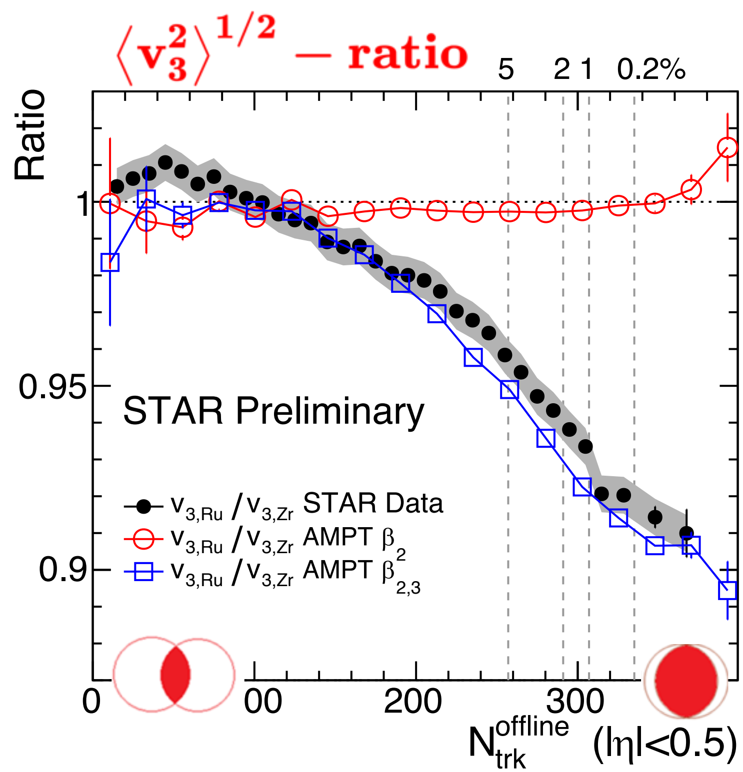

Nuclear structure via v_2-ratio and v_3-ratio

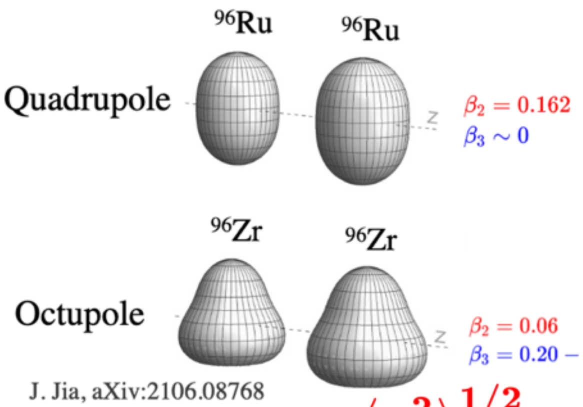

- β_{2Ru}~0.16 increase v_2, no influence on v_3 ratio
- β_{3Zr}~0.2 decrease v_2 in mid-central, decrease v_3 ratio
- Δa_0= -0.06fm increase v_2 mid-central, small impact on v_3.

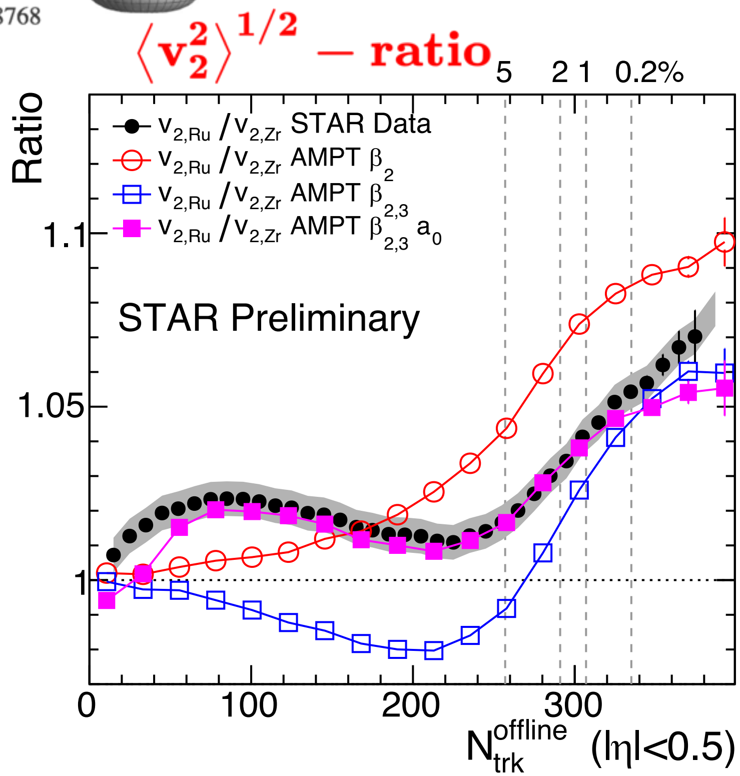

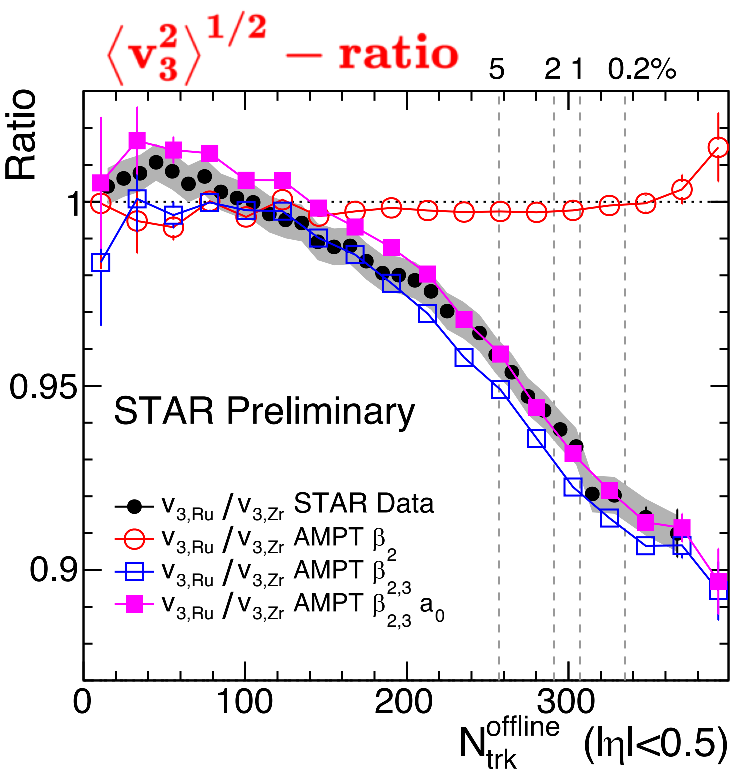

Nuclear structure via v_2-ratio and v_3-ratio

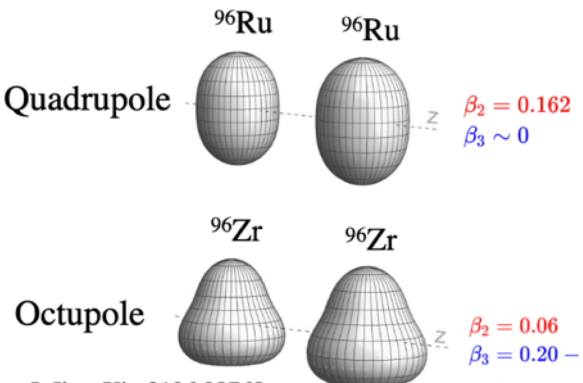

J. Jia, aXiv:2106.08768

- β_{2Ru}~0.16 increase v_2, no influence on v_3 ratio
- β_{3Zr}~0.2 decrease v_2 in mid-central, decrease v_3 ratio
- Δa_0= -0.06fm increase v_2 mid-central, small impact on v_3.
- Radius ΔR_0=0.07fm only slightly affects v_2 and v_3 ratio.

$$R_{\mathcal{O}} \equiv \frac{\mathcal{O}_{\mathrm{Ru}}}{\mathcal{O}_{\mathrm{Zr}}} \approx 1 + c_1\Delta\beta_2^2 + c_2\Delta\beta_3^2 + c_3\Delta R_0 + c_4\Delta a$$

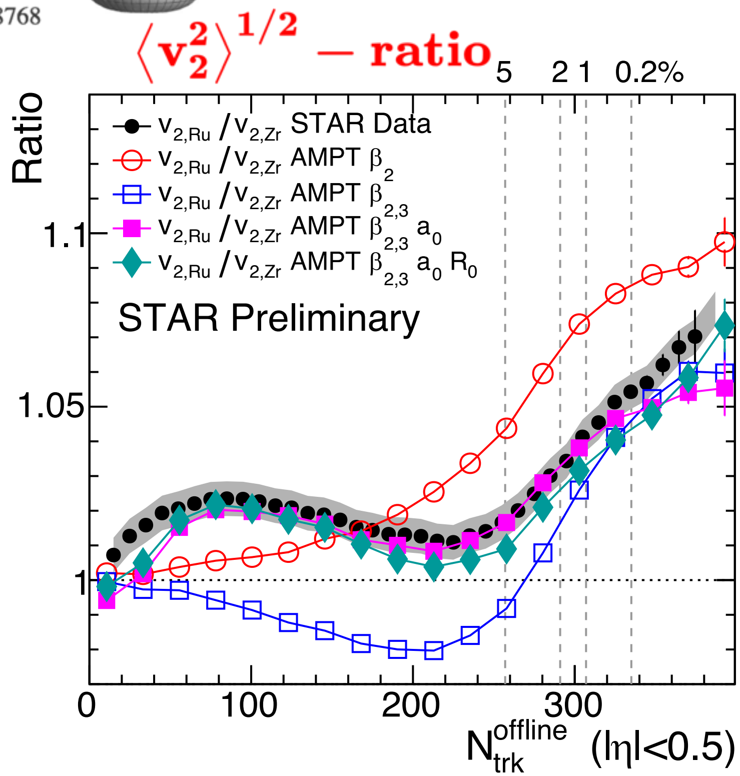

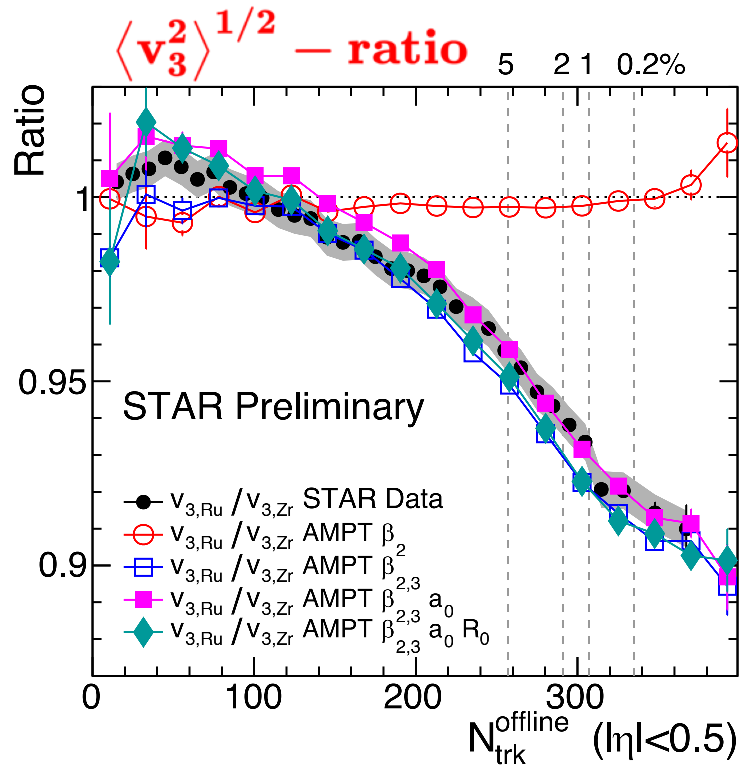

Simultaneously constrain these parameters using different N_{ch} regions

Isobar ratios cancel final state effects

- Vary the shear viscosity via partonic cross-section
  - Flow signal change by 30-50%, the v_n ratio unchanged.

$$v_n = k_n \varepsilon_n$$

$$\frac{v_{n,\mathrm{Ru}}}{v_{n,\mathrm{Zr}}} \approx \frac{\varepsilon_{n,\mathrm{Ru}}}{\varepsilon_{n,\mathrm{Zr}}}$$

Robust probe of initial state!

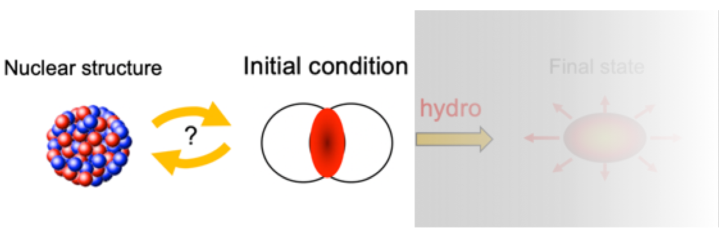

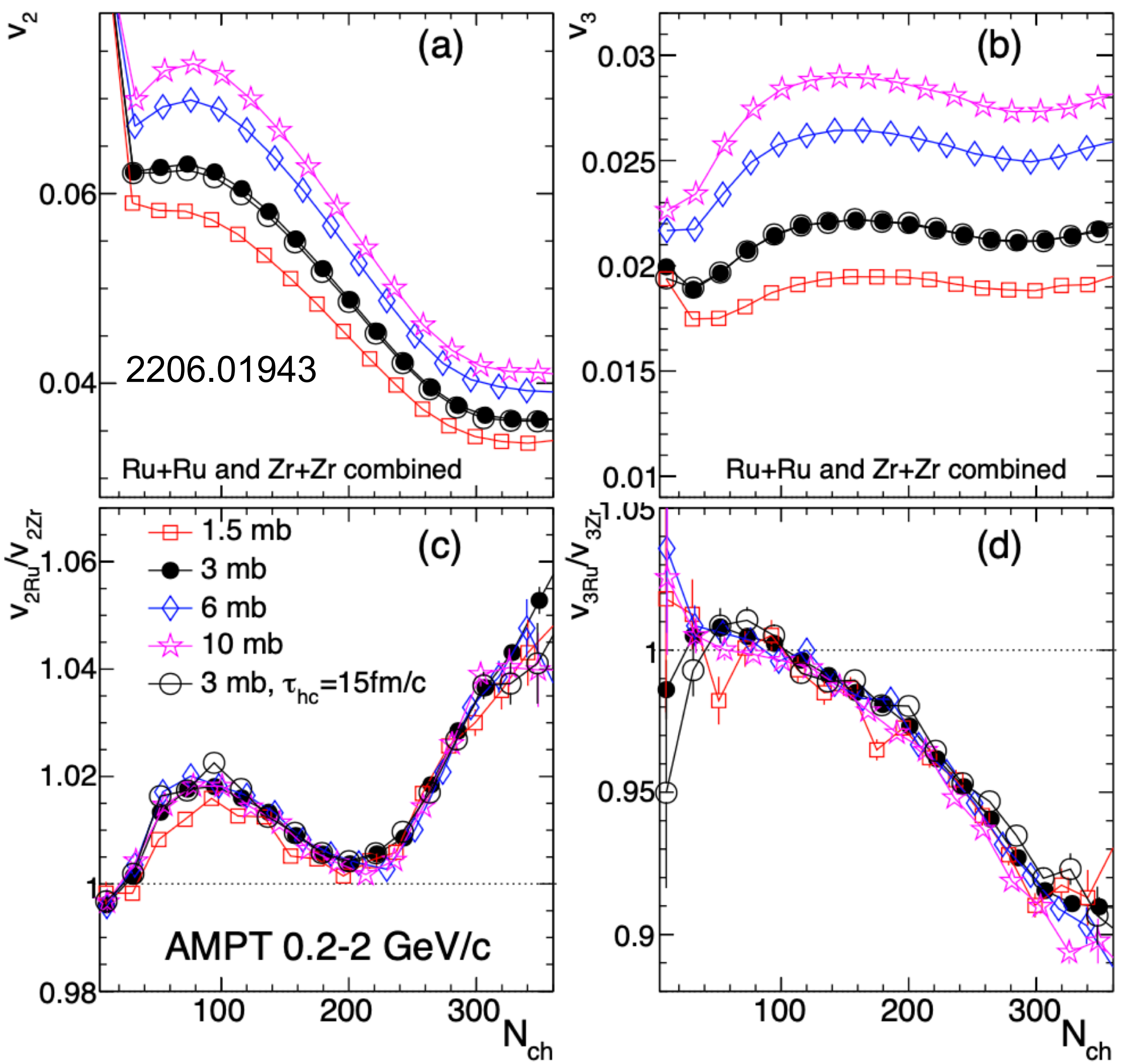

Triaxiality

$$R(\theta,\phi) = R_0\left(1 + \beta_2[\cos\gamma Y_{2,0} + \sin\gamma Y_{2,2}]\right.$$

1910.04673, 2004.14463

Prolate

$\beta_2 = 0.25, \cos(3\gamma) = 1$

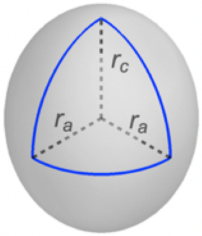

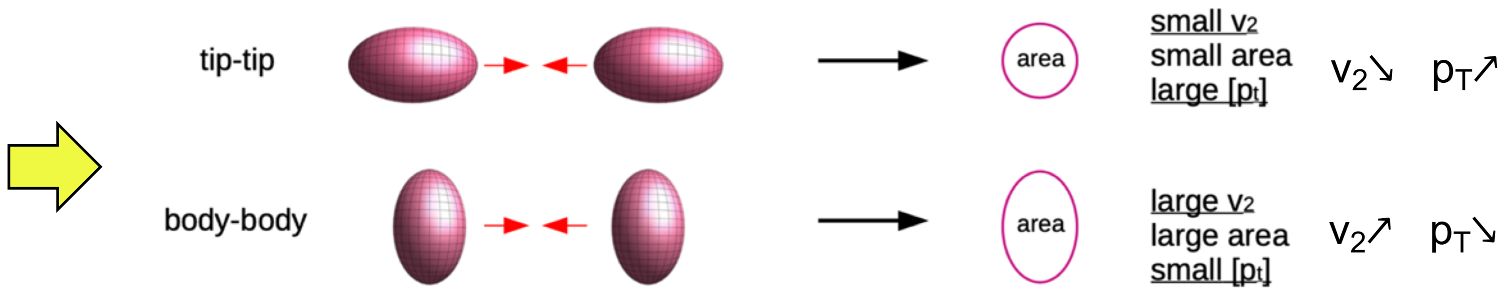

Need 3-point correlators to probe the 3 axes

$$\langle v_2^2 \delta p_{\mathrm{T}} \rangle \sim -\beta_2^3 \cos(3\gamma) \qquad \langle (\delta p_{\mathrm{T}})^3 \rangle \sim \beta_2^3 \cos(3\gamma)$$

2109.00604

Triaxial

$\beta_2 = 0.25, \cos(3\gamma) = 0$

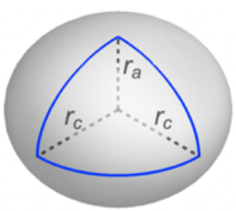

Oblate

$\beta_2 = 0.25, \cos(3\gamma) = -1$

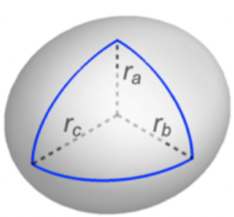

Triaxiality

$$R(\theta,\phi) = R_0\left(1 + \beta_2[\cos\gamma Y_{2,0} + \sin\gamma Y_{2,2}]\right.$$

1910.04673, 2004.14463

Prolate

$\beta_2 = 0.25, \cos(3\gamma) = 1$

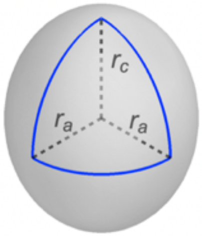

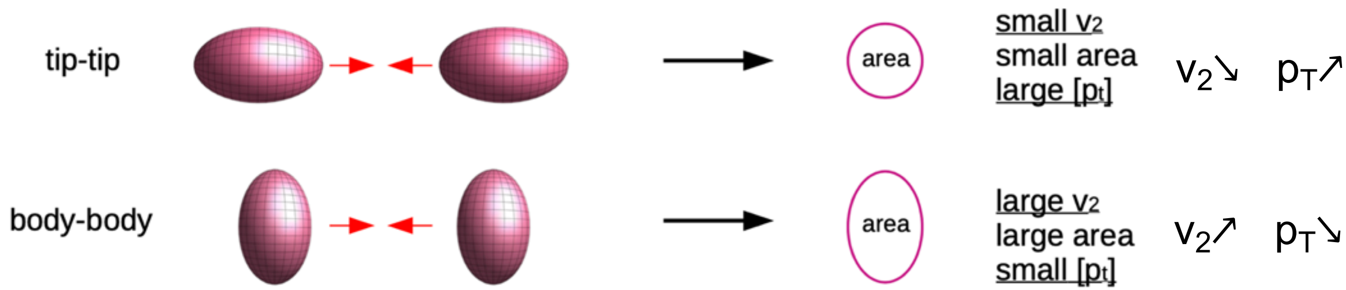

Need 3-point correlators to probe the 3 axes

$$\langle v_2^2\delta p_T\rangle \sim -\beta_2^3\cos(3\gamma) \qquad \langle(\delta p_T)^3\rangle \sim \beta_2^3\cos(3\gamma)$$

2109.00604

Triaxial

$\beta_2 = 0.25, \cos(3\gamma) = 0$

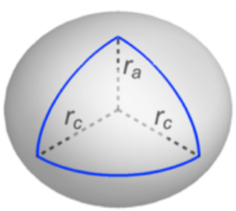

Compare U+U vs Au+Au: $\beta_{2U} \sim 0.28$, $\beta_{2Au} \sim 0.13$:

Oblate

$\beta_2 = 0.25, \cos(3\gamma) = -1$

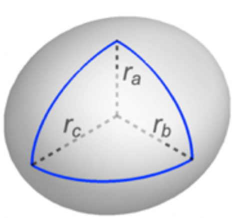

v_2-$[p_T]$ covariance

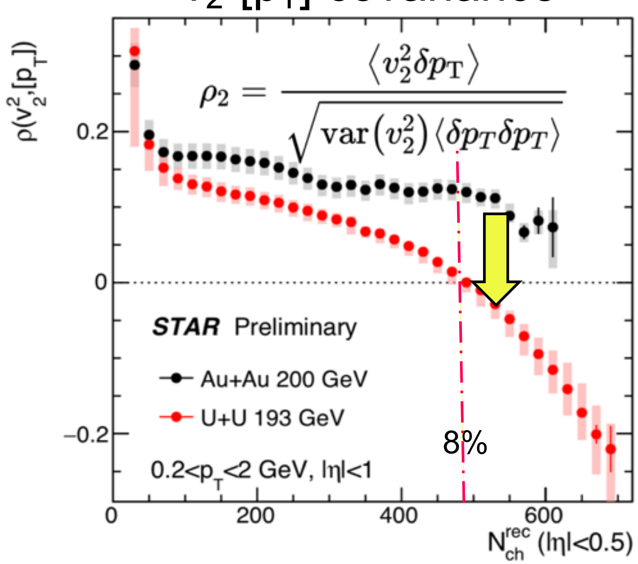

$[p_T]$ skewness

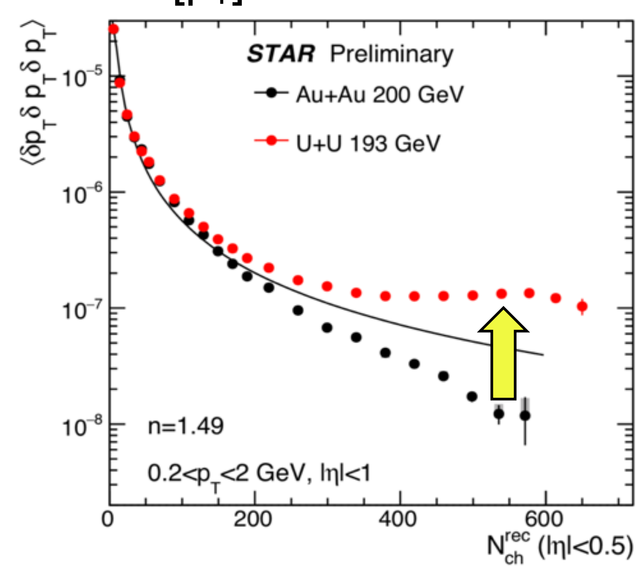

https://arxiv.org/abs/2209.11042

[Submitted on 22 Sep 2022]

Imaging the initial condition of heavy-ion collisions and nuclear structure across the nuclide chart

Benjamin Bally, James Daniel Brandenburg, Giuliano Giacalone, Ulrich Heinz, Shengli Huang, Jiangoyng Jia, Dean Lee, Yen-Jie Lee, Wei Li, Constantin Loizides, Matthew Luzum, Govert Nijs, Jacquelyn Noronha-Hostler, Mateusz Ploskon, Wilke van der Schee, Bjoern Schenke, Chun Shen, Vittorio Somà, Anthony Timmins, Zhangbu Xu, You Zhou

A major goal of the hot QCD program, the extraction of the properties of the quark gluon plasma (QGP), is currently limited by our poor knowledge of the initial condition of the QGP, in particular how it is shaped from the colliding nuclei. To attack this limitation, we propose to exploit collisions of selected species to precisely assess how the initial condition changes under variations of the structure of the colliding ions. This knowledge, combined with event-by-event measures of particle correlations in the final state of heavy-ion collisions, will provide in turn a new way to probe the collective structure of nuclei, and to confront and exploit the predictions of state-of-the-art ab initio nuclear structure theories. The US nuclear community should capitalize on this interdisciplinary connection by pursuing collisions of well-motivated species at high-energy colliders.

III. Science cases at the intersection of nuclear structure and hot QCD

A. Stress-testing small system collectivity with ^{20}Ne

B. Shape evolution along the Samarium isotopic chain

C. The neutron skin of ^{48}Ca and ^{208}Pb in high-energy collisions

D. Initial conditions of heavy-ion collisions

E. Impact on future experiments: EIC and CBM FAIR

Summary and outlook

- Collective flow response to collision geometry provide a tool to image nuclear shape at ultra-short time scale 10^{-24}s. Measurement of many-particle correlation in momentum space probes the many-nucleon correlations in the configuration space.
- Manifestation of nuclear shape at high-energy/shorter time-scale might be different from low energy (gluon saturation and nuclear PDF effects).
- Collisions of carefully-selected isobar species (at LHC) help us to understand the many-body nucleon correlations of atomic nuclei from small to large system & help constrain the heavy ion initial condition

A	isobars	A	isobars	A	isobars	A	isobars	A	isobars	A	isobars
36	Ar, S	80	Se, Kr	106	Pd, Cd	124	Sn, Te, Xe	148	Nd, Sm	174	Yb, Hf
40	Ca, Ar	84	Kr, Sr, Mo	108	Pd, Cd	126	Te, Xe	150	Nd, Sm	176	Yb, Lu, Hf
46	Ca, Ti	86	Kr, Sr	110	Pd, Cd	128	Te, Xe	152	Sm, Gd	180	Hf, W
48	Ca, Ti	87	Rb, Sr	112	Cd, Sn	130	Te, Xe, Ba	154	Sm, Gd	184	W, Os
50	Ti, V, Cr	92	Zr, Nb, Mo	113	Cd, In	132	Xe, Ba	156	Gd,Dy	186	W, Os
54	Cr, Fe	94	Zr, Mo	114	Cd, Sn	134	Xe, Ba	158	Gd,Dy	187	Re, Os
64	Ni, Zn	96	Zr, Mo, Ru	115	In, Sn	136	Xe, Ba, Ce	160	Gd,Dy	190	Os, Pt
70	Zn, Ge	98	Mo, Ru	116	Cd, Sn	138	Ba, La, Ce	162	Dy,Er	192	Os, Pt
74	Ge, Se	100	Mo, Ru	120	Sn, Te	142	Ce, Nd	164	Dy,Er	196	Pt, Hg
76	Ge, Se	102	Ru, Pd	122	Sn, Te	144	Nd, Sm	168	Er,Yb	198	Pt, Hg
78	Se, Kr	104	Ru, Pd	123	Sb, Te	146	Nd, Sm	170	Er,Yb	204	Hg, Pb

arXiv:2102.08158

TABLE I. Pairs and triplets of stable isobars (half-life > 10^8 y). 141 nuclides are listed. The region marked in red contains large strongly-deformed nuclei ($\beta_2 > 0.2$). The region marked in blue corresponds to nuclides which may present an octupole deformation in their ground state [48].